JOURNAL OF SOLID STATE CHEMISTRY 68, 273–284 (1987)

Relationship between Oxygen Self-Diffusion and Debye Temperature in the Polycrystalline Magnesium Aluminum Ferrite Series, $MgAl_{2-x}Fe_xO_4$

H. HANEDA, H. YAMAMURA, A. WATANABE, AND S. SHIRASAKI

National Institute for Research in Inorganic Materials, Sakura-Mura, Niihari-Gun, Ibaraki 305, Japan

Received February 4, 1985; in revised form February 28, 1986

Self-diffusion coefficients of oxygen in a spinel solid solution system, $MgAl_{2-x}Fe_xO_4$, have been measured by a gas–solid isotope-exchange technique using ^{18}O as a tracer. Mössbauer spectra of the same spinel solid solution have been studied over the temperature range where the materials were paramagnetic. The line broadening characteristic of Mössbauer spectra of these materials was interpreted in terms of distribution of the electric field gradient at ^{57}Fe nuclei. Debye temperatures were calculated from the temperature dependence of the absorption intensity of their Mössbauer spectra. The compositional dependence of the Debye temperature from the Mössbauer effect followed that of the activation energy of diffusion. A linear relationship between the activation energy and the square of the Debye temperature exists.

1. Introduction

The activation energy and preexponential terms for oxygen volume self-diffusion in a solid are often influenced by impurities or dopants (*1*). In this case, the nature of chemical bonding is believed to change. In the present study, we have measured the oxygen diffusion coefficients of the $MgAl_{2-x}Fe_xO_4$, solid–solution system and the results are discussed in relation to the Debye temperature, determined from the Mössbauer effect as well as the characteristics of lattice dynamics.

It is well-known that the following empirical relation holds for vacancies in metal systems which have the same crystal structures (*2*):

$$\Delta H_f = K \cdot m \cdot \theta_D^2 \cdot a^2, \qquad (1)$$

where ΔH_f is the monovacancy formation energy; m, the mass of constituent atoms; θ_D, the Debye temperature; a, the lattice constant; and K, a proportionality constant depending on the crystal structure. θ_D is defined as $\theta_D = h\nu_D/k$, where ν_D is the Debye frequency, so the dimension for $m\theta_D^2 \cdot a^2$ is energy. March (*3*) has shown that in metal system the proportionality between vacancy formation energy, ΔH_f, and θ_D^2 can be obtained using dielectric screening theory, to first order, to relate ΔH_f to the Fermi energy; Glyde (*4*) has shown that, in the Debye model, the dynamical theory of diffusion leads directly to a relation between $\Delta H = \Delta H_f + \Delta H_m$, where ΔH_m is migration energy, and the Debye temperature. According to Glyde, Eq. (1) should hold also in an ionic crystal. In the present study, the compositional dependence of the

0022-4596/87 $3.00

TABLE I

IMPURITY CONTENT OF STARTING MATERIALS

	Al	Si	Na	Mg	Mn	Fe	Co	Ni	Cu	Ca
Fe_2O_3	–	+	2	+	11	*	44	20	6	–
Al_2O_3	*	40	10	10	*	20	*	*	10	*
$Mg(OH)_2$#	30	140	5	*	*	15	*	*	*	55

Note. Values are in ppm. +, trace; –, not detected; *, no data; #, MgO base.

activation energy of oxygen diffusion is also interpreted on the basis of a modified form of Eq. (1).

2. Experimental

Polycrystalline $MgAl_{2-x}Fe_xO_4$ solid solutions (x = 0.0, 0.4, 0.8, 1.2, 1.6, and 2.0) were prepared by the usual ceramic method. The following were used as starting materials: 3 N $Mg(OH)_2$, 3 N Fe_2O_3, and 4 N Al_2O_3. Impurity levels are given in Table I. Desired amounts of these reagents were wet mixed and then calcined at 1100°C for a day in air. The resulting powder was milled and fired again under the same conditions. The products were milled, pelletized under a pressure of 2.0×10^8 Pa, and then finally fired at 1400°C for a week in air. $MgAl_2O_3$, however, was fired at 1700°C for a week in air because of the low reactivity and the sinterability of this material. The fired materials were quenched in air down to room temperature and crushed to particles, and these particles were screened with sieves for diffusion experiments. Some material was ground for X-ray diffraction and Mössbauer studies. The average grain sizes were determined on the basis of SEM in usual way and are given in Table II. X-ray diffraction showed that these materials were monophasic spinel compounds. In the present system, a second phase like MgO was detectable by X-ray up to a limit of 0.5%. This amount of second phase does not influence the value of the oxygen diffusion coefficient, because oxygen diffusivity is very low in MgO or Al_2O_3 and the exchange amount is larger in the present study. The resultant lattice constants are also presented in Table II.

The Debye temperature was determined from the temperature dependence of the absorption intensity in the Mössbauer spectra. These were recorded at varying temperatures using a Mössbauer spectrometer (Elscient Co.) in a constant acceleration mode. A proportional counter was used as a detector and ^{57}Co in Pd, at room temperature, was used as a source. The velocity scale was calibrated with an iron foil.

The self-diffusion coefficients of oxygen in a $MgAl_{2-x}Fe_xO_4$ solid solution were determined by measuring the rate of gas–solid exchange of ^{18}O at various temperatures in oxygen gas enriched with 5–20% ^{18}O at a pressure of about 5.3×10^3 Pa. The reaction chamber was equipped with a Pt–20% Rh susceptor and a Pt–20% Rh crucible, which were heated by a high-frequency induction method. The volume of the gas phase was 300 cm^3. The reaction chamber was evacuated to a pressure of about 1×10^{-1} Pa. Then ^{18}O-enriched oxygen gas was introduced into the chamber. Prior to each diffusion annealing, the system was preheated at 700 ~ 900°C for 15 min. The exchange process as a function of diffusion time was followed by analyzing the ^{18}O content of the gaseous phase with a mass spectrometer. Details of the experimental setup and procedures have already been de-

TABLE II

CRYSTAL PROPERTIES FOR $MgAl_{2-x}Fe_xO_4$

	Compositional parameter, x	Grain radius (μm)	Lattice constant, a (nm)	Debye temperature (K)	Average reduced mass (amu units)
A	0.0	8.3	0.8083	520	9.92
B	0.4	6.8	0.8141	510	10.43
C	0.8	5.7	0.8204	483	10.86
D	1.2	3.6	0.8272	409	11.23
E	1.6	1.3	0.8331	403	11.55
F	2.0	3.1	0.8356	397	11.86

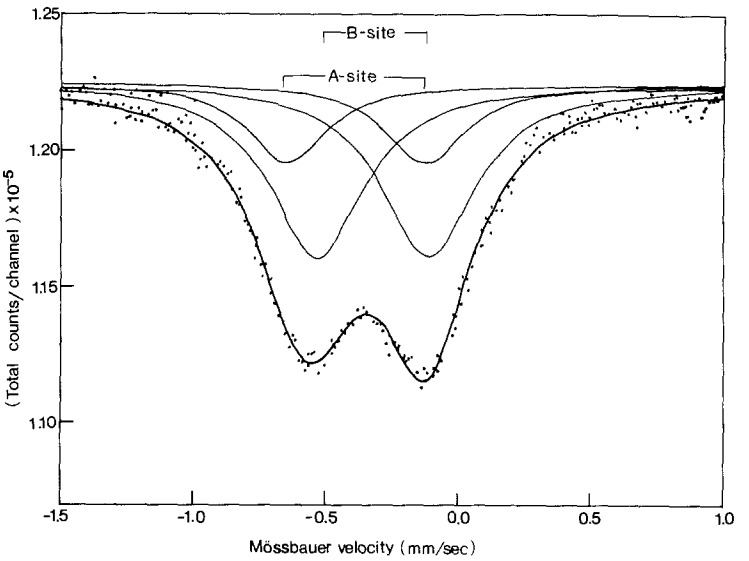

FIG. 1. Mössbauer spectra of $MgFe_2O_4$ at 1185°C.

scribed by Oishi and Kingery (*5*). If the diffusion process controls the exchange reaction ($C_{gas}(t) = C_{surface}(t)$, $C_{gas}(t)$ = isotope concentration in gas phase at any time, t, $C_{surface}(t)$ = isotope concentration at the sample surface at the same time), the total amount of ^{18}O, M_t, in the sphere sample after time, t, is expressed as a fraction of corresponding quantity, M_∞, after infinite time by the equation (*6*):

$$\frac{M_t}{M_\infty} = (1+\alpha)\Big[1 - \frac{\gamma_1}{\gamma_1+\gamma_2}\,eerfc\left\{\frac{3\gamma_1}{\alpha}\left(\frac{Dt}{A^2}\right)^{1/2}\right\} - \frac{\gamma_2}{\gamma_1+\gamma_2}\,eerfc\left\{-\frac{3\gamma_2}{\alpha}\left(\frac{Dt}{A^2}\right)^{1/2}\right\}\Big] + \text{higher terms}$$

$$\gamma_1 = \tfrac{1}{2}\{(1+\tfrac{4}{3}\alpha)^{1/2}+1\},\quad \gamma_2 = \gamma_1 - 1$$

$$eerfc(z) = \exp(z^2)[1 - erf(z)]$$

$$erf(z) = 2/\pi^{1/2}\int_0^z \exp(-\eta^2)d\eta \qquad (2)$$

where A is radius of the sample and α is the gram ratio of oxygen present in the solid to that in the gaseous phase. According to the result studied by Carman and Haul, the next two higher terms have opposite signs, so the influence of these terms is very small (*6*). The error of Eq. (2) caused by neglecting the higher term is, experimentally, less than 2% (*7*). Calculations of diffusion coefficients in the present study, therefore, were done using Eq. (2). In the determination of oxygen lattice diffusion in polycrystalline $MgAl_{2-x}Fe_xO_4$ solid solutions, the method (*8*) proposed by Shirasaki *et al.* was applied.

3. Result and Discussions

a. Mössbauer effects

Figure 1 shows the Mössbauer spectra of $MgFe_2O_4$ at 1185°C, the temperature at which the material was in a paramagnetic state; the spectra consist of a diffuse asymmetrical doublet. The calculated doublets (both with the Lorentzian line shape) are also shown in Fig. 1. As seen there, an isomer shift of the doublet with weaker intensity is smaller than that of the one with

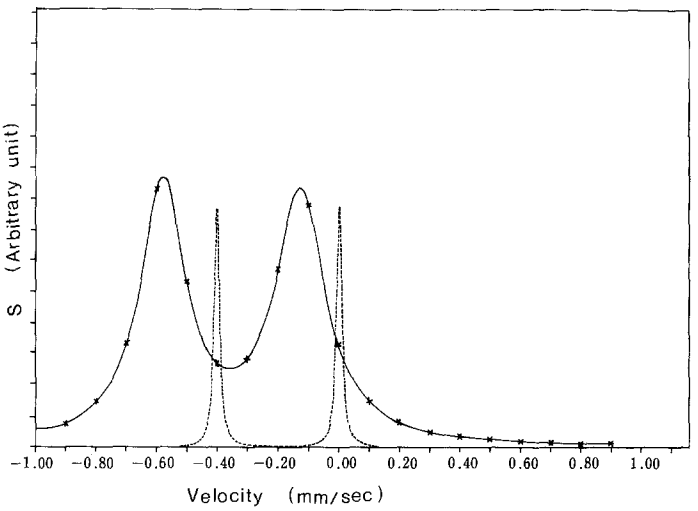

FIG. 2. Distribution of electric environment in Mössbauer spectra of $MgFe_2O_4$ and $ZnFe_2O_4$. Solid line with crosses, $MgFe_2O_4$; dashed line, $ZnFe_2O_4$.

stronger intensity, so that the former is due to Fe^{3+} in a tetrahedral (A) site, the latter, in an octahedral (B) site (*9*).

These linewidths were about twice as broad as the linewidth of a pure iron foil ($= 2.2 \times 10^{-4}$ m/sec). The degree of the broadening was estimated on the basis of a deconvolution of Mössbauer spectra. Figure 2 shows the results of this analysis. The linewidth of $MgAl_{2-x}Fe_xO_4$ was broader than that of a completely normal spinel, $ZnFe_2O_4$, measured at 298 K. Mössbauer line broadening with a mechanism of the hopping ($Fe^{2+} \leftrightarrow Fe^{3+}$) or the diffusion of iron ions are sensitive to a change of temperature (*10*). However, in the present materials line broadening was independent of temperature, so we can say that the line broadening seen in $MgAl_{2-x}Fe_xO_4$ is associated with the occurrence of a random distribution of constituent ions, Mg^{2+}, Al^{3+}, and Fe^{3+}, over two different cation sites of the spinel structure. This mechanism has been found in perovskite structure (*11*).

In the present study, the recoilless fraction and the Debye temperature of $MgAl_{2-x}Fe_xO_4$ were determined by measuring the temperature dependence of the total area intensity of two doublets. Consequently, the resulting values are regarded as an average of A-site and B-site ferric ions. The area intensity, A_r, can be expressed by the equation (*12*):

$$A_r \cong K \cdot f \cong K \cdot \exp\left[-\frac{3E_R}{2k\theta_D}\{1 + 4(1/Z)^2 Z(1 - Z/4 + Z^2/36 - Z^4/3600)\}\right], \quad Z = \theta_D/T, \quad (3)$$

where K is a factor containing terms such as the amount of the Mössbauer nuclei, γ-ray cross section, and so on; f, the recoilless fraction; E_R, the recoil energy; θ_D, the Debye temperature; and T, the temperature of sample. Figure 3 shows the temperature dependence of the absorption intensity in $MgFe_2O_4$. Open circles are the observed data points and the solid curve is drawn to fit these data points using Eq. (3). The success of the curve-fitting procedure implies that the application of the Debye model to the temperature dependence of the absorption intensity is reasonable in these materials.

Figure 4 shows the compositional dependence of the Debye temperature from the

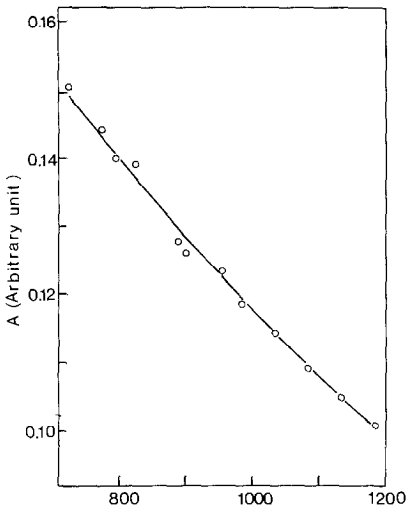

FIG. 3. The temperature dependence of absorption area intensity for $MgFe_2O_4$. Open circles, experimental results; solid line, calculated values.

recoilless fraction. As seen in Fig. 4, the Debye temperature decreases with increasing compositional parameter, x, and drastically changes at $x = 1.0$. This tendency was also encountered in the Debye temperature obtained from the neutron diffraction data from this system (*13, 14*) (see Fig. 4). The Debye temperatures obtained from the Mössbauer effect are lower than those from

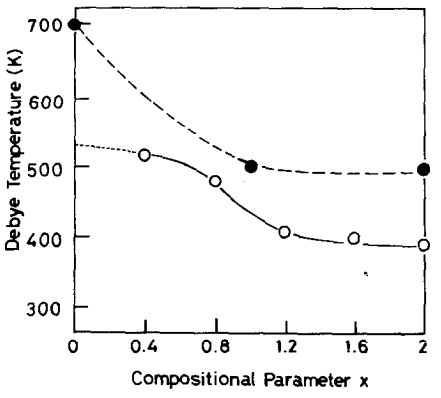

FIG. 4. Debye temperature as a function of x in $MgAl_{2-x}Fe_xO_4$. O, present study; ●, neutron diffraction data.

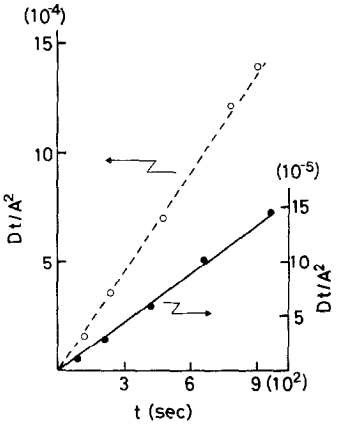

FIG. 5. Plots of Dt/A^2 versus time. O, polycrystalline $MgFe_2O_4$ (1345°C, 24 μm particle size); ●, polycrystalline $MgFe_{1.6}Al_{0.4}O_4$ (1298°C, 24 μm).

neutron diffraction, because the Mössbauer effect is more sensitive to the acoustical modes of lattice vibration than optical modes, which generally have higher frequencies. The Debye temperature of $MgAl_2O_4$ doped with ^{57}Fe could not be obtained accurately, so an extrapolated value, 520 K, was used in the present study.

b. Oxygen Self-diffusion

Figure 5 shows typical time dependences of the dimensionless quantity, Dt/A^2, which were determined using Eq. (2) in polyacrystalline $MgFe_2O_4$ and $MgFe_{1.6}Al_{0.4}O_4$. Both plots are fit by straight lines passing through the origin, indicating that the surface exchange kinetics between gas and the solid surface ($C_{gas}(t) > C_{surface}(t)$) was not controlled by rate, but that diffusion within the solid controlled the exchange reaction. The behavior of the other materials was the same. The apparent diffusion coefficient was calculated from the slope of this line.

Figure 6 shows the temperature dependence of apparent oxygen diffusion coefficients of polycrystalline $MgAl_{2-x}Fe_xO_4$ (with A = particle size from sieves in Eq. (2)). As seen there, the apparent activation energy increases with particle size on the

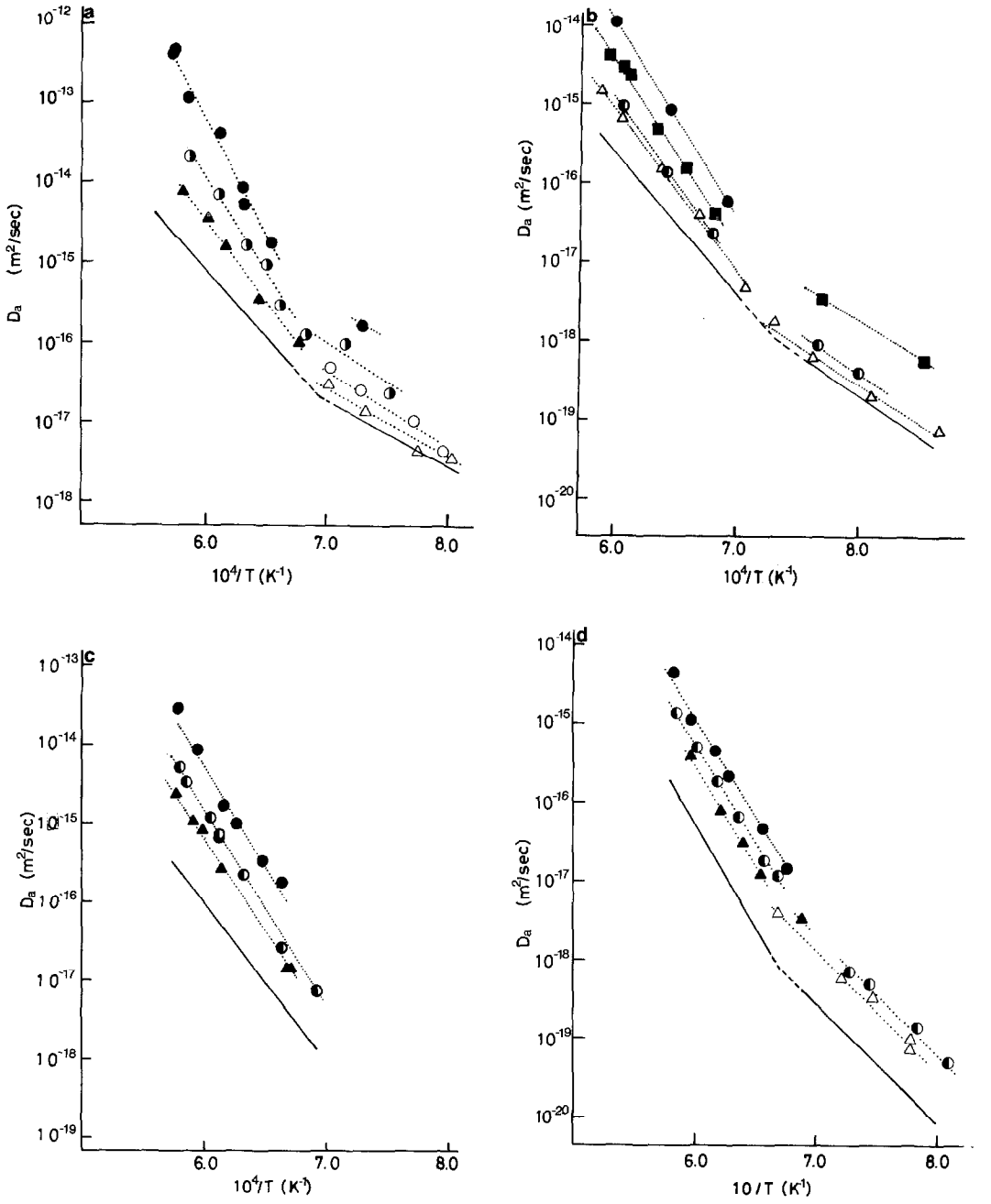

FIG. 6. The temperature dependence of apparent oxygen diffusion coefficients (· · ·) and volume diffusion coefficients (——). (a) x (compositional parameter) = 2.0; (b) 1.6; (c) 1.2; (d) 0.8; (e) 0.0. ●, 540 μm; ■, 178 μm; ◑, 135 μm, ◐, 105 μm; ○, 57 μm; ▲, 48 μm; △, 24 μm.

Fe side of the compositional range. This tendency was not found in $MgAl_{1.2}Fe_{0.8}O_4$, which has fewer iron ions than $MgFe_2O_4$ (see Fig. 6). Generally speaking, the apparent activation energy of oxygen diffusion does not depend on particle size, or it in-

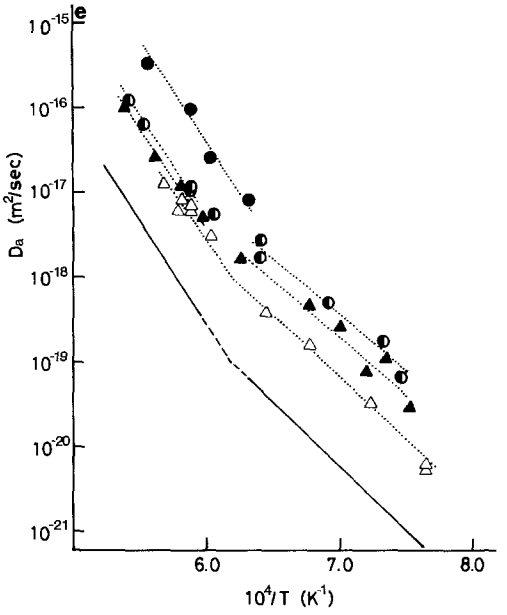

FIG. 6—*Continued.*

creases with decreaing particle size as in Mg_2TiO_4 (*8*). This anomaly shows that the relative magnitude of D_b (grain-boundary diffusion coefficient) compared to D_l (lattice diffusion coefficient) increases with increasing temperature and that the activation energy for D_b is larger than that of D_l. The distribution of cations at the B site at the grain boundary do not contribute to this behavior, because $MgAl_2O_4$ with normal spinel structure and Mg_2TiO_4 with inverse spinel structure also have normal behavior (*8*). Paulus claimed the occurrence of a preferential reduction in the grain-boundary region with increasing temperature in Mn–Zn ferrite (*15*). In the present materials, at the Fe-rich side of the compositional range, the reduction of Fe ion and the formation of oxygen vacancies may occur preferentially along grain boundaries at elevated temperatures. As a result oxygen diffusion at grain boundary becomes considerable. In this view, the resultant diffusion coefficients using Eq. (2) are apparent in polycrystalline materials.

The lattice diffusion coefficient was determined by a method proposed by Shirasaki *et al.* (*8*). Figure 7 shows typical plots of log(particle radius) against log(D_a) of present materials which were calculated for cases of A = particle size (Eq. (2)). As seen there, all calculations give straight lines. When A = particle radius, a positive slope is obtained. If straight lines can be extrapolated to the point of the grain radius, the apparent diffusion coefficient at the grain radius should correspond to the volume diffusion coefficient, because at this point the effect of grain-boundary diffusion is absent. Lattice diffusion coefficients were calculated from all experimental data in the same region by a least-squares method. The resulting lattice diffusion coefficients are also shown in Fig. 6. Figure 8 shows the lattice diffusion coefficients of single and polycry-

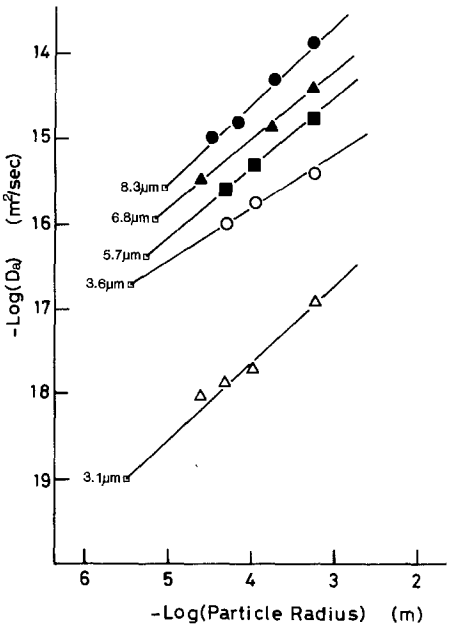

FIG. 7. Particle size dependence of the apparent diffusion coefficients calculated for A = grain radius in $MgAl_{2-x}Fe_xO_4$. ●, $MgFe_2O_4$; ▲, $MgFe_{1.6}Al_{0.4}O_4$; ■, $MgFe_{1.2}Al_{0.8}O_4$; ○, $MgFe_{0.8}Al_{1.2}O_4$; △, $MgAl_2O_4$. Values of apparent diffusion coefficients at small squares; volume diffusion coefficients.

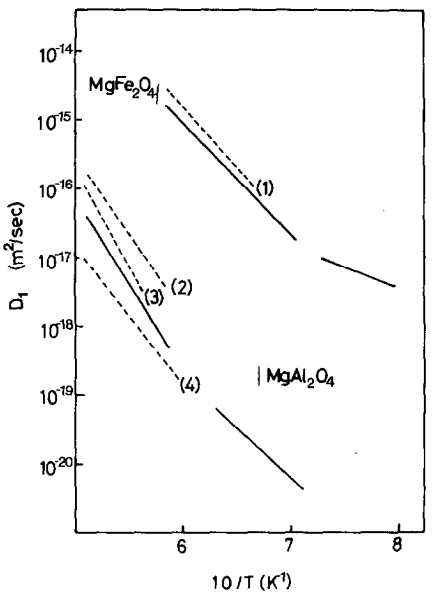

FIG. 8. Oxygen volume diffusion coefficients for $MgFe_2O_4$ and $MgAl_2O_4$ for polycrystal (present work) (——), and single crystal (– – –). 1, Ref. (*7*); 2, Ref. (*21*); 3, Ref. (*20*); 4, Ref. (*22*).

stals of $MgAl_2O_4$ and $MgFe_2O_4$. The values obtained from polycrystals in the higher temperature region agree with those of single crystals, so the method used in the present study is valid.

One can find two regions of behavior for polycrystals in Fig. 6. Dieckmann and Schmalzried (*16*) claimed that the dominant disorder of magnetite, which has a spinel-type structure, was a cation vacancy at higher oxygen partial pressure and was the "Frenkel" type at lower oxygen pressure. Spinel-type structures have many interstitial cation sites. However, the oxygen ion sublattice is rather close-packed compared to the cation sublattice, and the radius of interstitial sites (≅0.4 Å) is much smaller than that of oxygen ion (≅1.4 Å). Also, results of the theoretical works (*17, 18*) indicate that vacancies are the dominant disorder in close-packed structures. Hence a vacancy-type defect is probable for oxygen diffusion in the present materials. It is likely that the high-temperature and the low-temperature regions are due to intrinsic and extrinsic diffusion, respectively. Under the above-mentioned assumption, the enthalpy of vacancy formation, ΔH_f, was calculated from the activation energy of the intrinsic (ΔH_i) and the extrinsic (ΔH_m) regions ($\Delta H_f = \Delta H_i - \Delta H_m$). The values of ΔH_i, ΔH_m, ΔH_f, and preexponential terms, D_0, for oxygen diffusion in $MgAl_{2-x}Fe_xO_4$ are summarized in Table III. The estimated errors are less than 20 kJ/mole, so the preexponential terms have less error than a one-quarter order of magnitude. As seen in Table III, the D_0 value of $MgAl_{1.2}Fe_{0.8}O_4$ at intrinsic region is greater than those of $MgFe_2O_4$ and $MgAl_2O_4$, which are end members of these solid solutions. D_0 has a physical meaning which can expressed as

$$D_0 = K' \cdot a^2 \cdot \nu \cdot \exp((\Delta S_f + \Delta S_m)/R), \quad (4)$$

where K' is the proportional constant due to structure, mechanism and so on; a is the lattice constant; ν is the vibration frequency of atom, generally taken as the Debye frequency; and ΔS_f and ΔS_m are the entropies of vacancy formation and vacancy migration, respectively. It is not expected that the values of K', a, and ν change by some orders of magnitude from sample to sample. Hence, the greatest value of D_0 at intermediate composition is due to change in the entropy terms.

c. Relation between Activation Energy and Debye Temperature

The activation energy in the intrinsic region changed remarkably when the compositional parameter $x = 1.0$. This shows a tendency similar to the compositional dependence of the Debye temperature obtained from measurement of the Mössbauer effect. Also there exists a relation between the activation energy of diffusion and the Debye temperature in oxide systems which is analogous to the case of metal systems.

TABLE III

OXYGEN DIFFUSION PARAMETERS FOR $MgAl_{2-x}Fe_xO_4$

Sample name:	A	C	D	E	F
Compositional parameter, x:	0.0	0.8	1.2	1.6	2.0
		High-temperature region			
D_0 (m^2/sec)	1.23×10^{-4}	2.08×10^{-1}	1.33×10^{-4}	9.65×10^{-6}	1.52×10^{-5}
ΔH_i (kJ/mole)	467	496	387	338	328
		Low-temperature region			
D_0 (m^2/sec)	2.21×10^{-10}	1.70×10^{-8}	—	4.10×10^{-11}	1.2×10^{-11}
ΔH_m (kJ/mole)	289	295	—	197	159
		Formation energy			
ΔH_f ($H_i - H_m$)	178	201	—	141	169
		Fitted value from Eq. (6)			
ΔH_{fc}	189 (400[a])	186	153	154	154
ΔH_{mc}	307	270	187	184	178
ΔH_{ic} ($H_{fc} + H_{mc}$)	496	456	340	338	332

[a] Calculated value (Ref. (*18*)).

Usually, the energy of vacancy formation or migration is calculated by the Shell model (*17*) for ionic crystals. This treatment has been reported for $MgAl_2O_4$ by Catlow *et al.* (*18*). In the present case, the application of the shell model is difficult, because the random distribution of cations and the dielectric constant and the elastic moduli have not been obtained. Hence, we examined the result using a more empirical Eq. (1). It is well-known that an empirical linear relationship between the energies for defect formation or migration and melting points exists (*19*). Furthermore, the melting points are proportional to the square of the Debye temperature (*2*). For the present study, the average values of reduced mass, $M_c \cdot M_o/(M_c + M_o)$, where M_c is the mass of cation (Mg, Al, or Fe) and M_o is the mass of oxygen ion, for ΔH_f and oxygen mass for ΔH_m were used in a modified form of Eq. (1), because ΔH_f is concerned with the whole lattice and ΔH_m with the neighboring oxygen of vacancy, respectively. These choices were confirmed by our calculation of halides (see Appendix).

The following equations show results which were obtained, when Eq. (1) was applied to the present spinels. Figures 9a and 9b show the result of the fitting procedure.

$$\Delta H_f \text{ (kJ/mole)} = 7.7 \times 10 \cdot M \cdot a^2 \cdot \theta_D^2 + 53.5 \quad \text{(formation)}$$

$$\Delta H_m \text{ (kJ/mole)} = 10.7 \times 10 \cdot M' \cdot a^2 \cdot \theta_D^2 - 33.5 \quad \text{(migration).} \quad (5)$$

In the calculation, we used the activation energy from the diffusion study and $m \cdot a^2 \cdot \theta_D^2$, where a is the lattice constant (Table II) and θ_D is the Debye temperature obtained from the Mössbauer effect (Fig. 5). Figure 10 shows the fitted and experimental values of intrinsic activation energy. These two values tend to agree with each other, so the treatment on the basis of the modified form of Eq. (1) can be applied to oxygen diffusion in the oxide system.

4. Conclusion

The Debye temperature of $MgAl_{2-x}Fe_xO_4$ spinel solid solutions was determined on

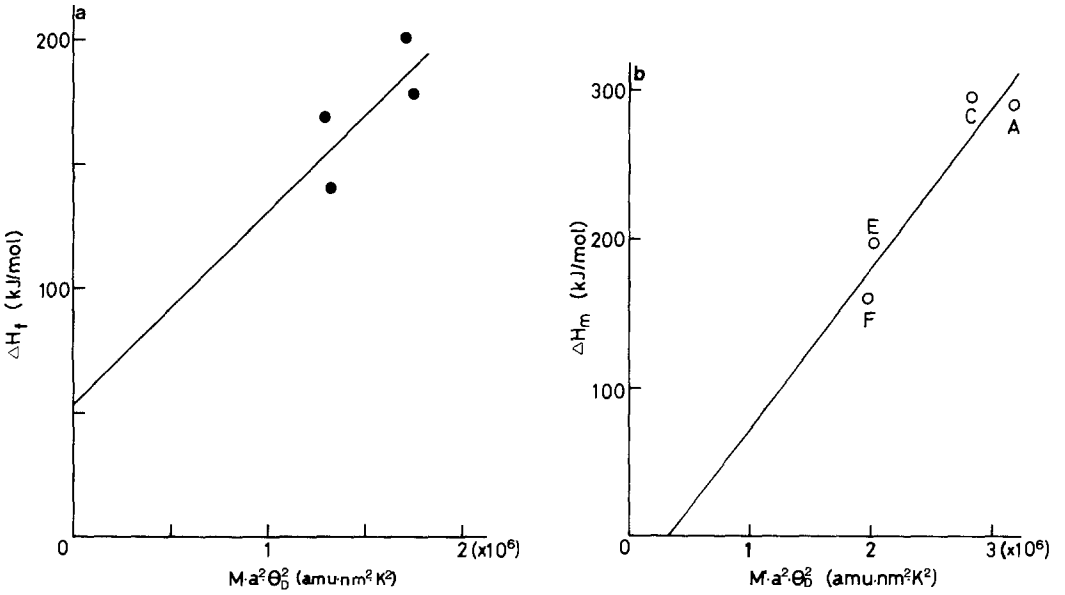

FIG. 9. Activation energy versus $M \cdot a^2 \cdot \theta^2$ and $M'' \cdot a^2 \cdot \theta^2$ for present materials. Activation energies of (a) vacancy formation and (b) migration.

the basis of the Mössbauer effect. The oxygen self-diffusion coefficient for the same composition was also measured. The intrinsic activation energy tends to follow the same dependence as the Debye temperature. A linear relationship exists between activation energy and square of the Debye temperature.

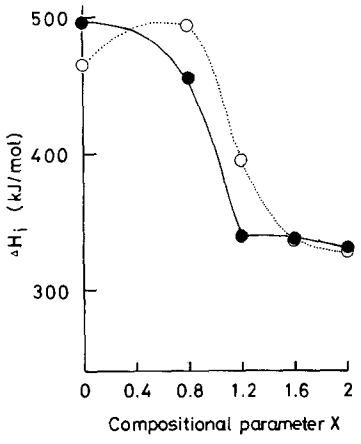

FIG. 10. Intrinsic activation energy of oxygen diffusion for $MgAl_{2-x}Fe_xO_4$. ○, observed values; ●, calculated values.

Appendix

In order to confirm the validity of the modified equation and choice of the mass, the modified form of Eq. (1) was applied to alkali halides having NaCl structure. Table AI shows correlation factors of least-squares fitting for various masses. As seen, the choice of the present study is the best

TABLE AI

CORRELATION FACTORS OF SOME LEAST-SQUARES FITTING PROCEDURES FOR ALKALI HALIDES

	M	M'	M''
ΔH_f	0.6914	—	0.1395
ΔH_m	0.0004	0.6785	0.0017

Note. M, reduced mass; M', mass of ion; M'', molecular weight.

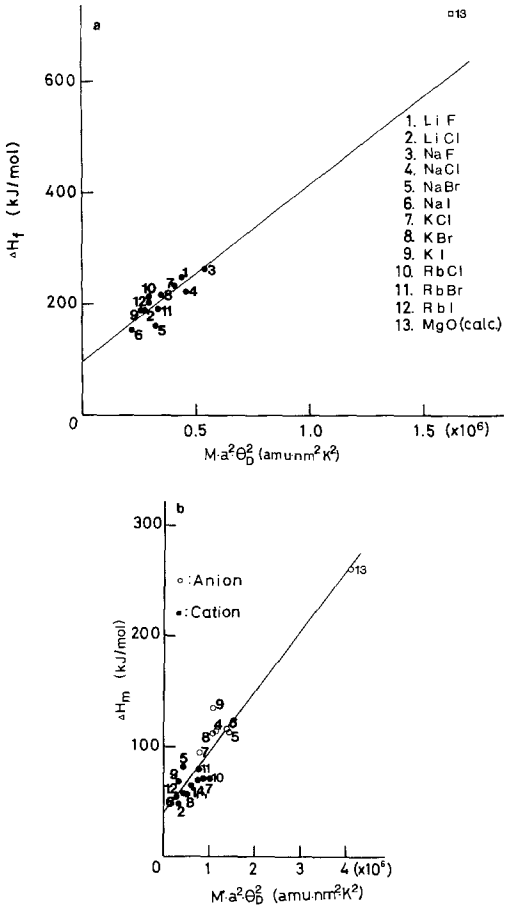

FIG. A1. Activation energy versus $M \cdot a^2 \cdot \theta_D^2$ and $M' \cdot a^2 \cdot \theta_D^2$ for alkali halides. H, in kJ/mol; M and M'', in amu units; a, in nm; θ_D in K. Activation energies for (a) vacancy formation and (b) migration. Debye temperatures, Ref. (*23*), activation energies, mean values of Refs. (*24*)–(*33*).

fitted. Figures A1a and A1b show the results for defect formation and migration, respectively. The Eq. (1) did not hold exactly but a linear relation was valid as follows (*23*):

$$\Delta H_f \text{ (kJ/mol)} = 31.8 \times 10^{-5} M \cdot a^2 \cdot \theta_D^2 + 98.1$$

$$\Delta H_m \text{ (kJ/mol)} = 5.45 \times 10^{-5} M' \cdot a^2 \cdot \theta_D^2 + 40.2,$$

where M is a reduced mass and M' is the mass of the diffusing ion in amu units. Extrapolated values nearly agree with those of MgO, which has the same structure, so this relation is considered to be applicable over a wide range.

References

1. S. SHIRASAKI, S. MATSUDA, H. YAMAMURA, AND H. HANEDA, *in* "Ceramic Advances," Vol. 12, in press.
2. K. MUKHERJEE, *Philos. Mag.* **12,** 915 (1965).
3. N. H. MARCH, *Phys. Lett.* **20,** 231 (1966).
4. H. R. GLYDE, *J. Phys. Chem. Solids* **28,** 2061 (1967).
5. Y. OISHI AND W. D. KINGERY, *J. Chem. Phys.* **33,** 480 (1960).
6. P. C. CARMAN AND R. A. W. HAUL, *Proc. R. Soc. A* **222,** 109 (1954).
7. H. HANEDA, I. SHINDO, H. YAMAMURA, AND S. SHIRASAKI, *J. Mater. Sci.* **19,** 2947 (1984).
8. S. SHIRASAKI, I. SHINDO, H. HANEDA, M. OGAWA, AND K. MANABE, *Chem. Phys. Lett.* **50,** 459 (1977).
9. E. DE GRAVE, C. DAUWE, J. DE SITTER, AND A. GOUAERT, *J. Phys. Colloq.* **37,** C6–467 (1976).
10. R. C. KAMAUER AND J. G. MULLER, *Phys. Rev.* **176** (1968).
11. R. O. BELL, *J. Phys. Chem. Solids* **29,** 1 (1968).
12. J. HEBERLE, *in* "Mössbauer Effect Methodology" (I. J. Gruverman, Ed.), Vol. 7, pp. 299–308, Plenum, New York (1977).
13. G. E. BACON, *Acta Crystallogr.* **5,** 684 (1952).
14. G. E. BACON AND F. F. ROBERTS, *Acta Crystallogr.* **6,** 57 (1953).
15. M. PAULUS, *in* "The Role of Grain Boundaries and Surfaces," "Materials Science Research" (W. W. Kriegel and H. Polmor III, Eds.), 31, Plenum, New York (1966).
16. R. DIECKMANN AND H. SCHMALZRIED, *Ber. Bunsenges. Physk. Chem.* **81,** 344 (1977); *Ber. Bunsenges, Physk. Chem.* **81,** 414 (1977).
17. W. C. MACKRODT, *in* "Computer Simulation of Solids" (C. R. A. Catlow and W. C. Mackrodt, Eds.), p. 175, Springer-Verlag, Berlin (1982).
18. C. R. A. CATLOW, M. DIXON, AND W. C. MACKRODT, *in* "Computer Simulation of Solids" (C. R. A. Catlow and W. C. Mackrodt, Eds.), p. 130, Springer-Verlag, Berlin (1982).
19. S. MROWEC, *in* "Defect and Diffusion in Solids," p. 110, Elsevier Scientific, New York (1980).
20. K. ANDO AND Y. OISHI, *J. Chem. Phys.* **61,** 625 (1974).
21. K. ANDO AND Y. OISHI, *Yogyo Kyokai Shi* **80,** 26 (1972).

22. K. P. R. REDDY AND A. R. COOPER, *J. Amer. Ceram. Soc.* **64,** 368 (1981).
23. D. E. GRAY (Ed), "American Institute of Physics Handbook," 3rd ed., pp. 4–115 and 4–116. McGraw–Hill, New York (1972).
24. L. W. BARR AND D. K. DAWSON, *in* "Mass Transport in Nonmetallic Solids: "Proceedings, British Ceramic Society," No. 19, p. 151 (1971).
25. P. KOFSTAD, *in* "Nonstoichiometry, Diffusion, and Electric Conductivity in Binary Metal Oxides," p. 55, Wiley–Interscience, New York (1972).
26. N. N. GREENWOOD, *in* "Ionic Crystals Lattice Defects and Nonstoichiometry, p. 76, Butterworths, London (1968).
27. C. P. FLYNN, *in* "Point Defects and Diffusion," p. 565, Oxford Univ. Press, London (1972).
28. W. C. MACKRODT, *in* "Computer Simulation of Solids" (C. R. A. Catlow and W. C. Mackrodt, Eds.), p. 175. Springer-Verlag, Berlin (1982).
29. M. SHARON AND R. R. PRADHANANGA, *J. Solid Sate Chem.* **40,** 20 (1981).
30. D. L. KIRK, *Phys. Status Solidi A* **54,** 251 (1979).
31. P. VAROTSOS, *Solid State Commun.* **25,** 583 (1978).
32. M. BENIERE, M. CHEMLA, AND F. BENIERE, *J. Phys. Chem. Solids* **37,** 525 (1976).
33. M. K. UPPAL, C. N. R. RAO, AND M. J. L. SANGATER, *Philos. Mag. A* **38,** 341 (1978).